Johann Radon Institute for
Computational and Applied Mathematics
Austrian Academy of Sciences (ÖAW)

Model function approach in the modified L-curve method for the choice of regularization parameter

Y. Heng, S. Lu, A. Mhamdi, S. Pereverzyev

RICAM-Report 2009-08

MODEL FUNCTION APPROACH IN THE MODIFIED L-CURVE METHOD FOR THE CHOICE OF REGULARIZATION PARAMETER

YI HENG[1], SHUAI LU[2], ADEL MHAMDI[1], SERGEI V. PEREVERZEV[2]

Abstract. The L-curve method is known as one of the most popular heuristic error-free regularization parameter choice rules in solving discrete ill-posed problems

$$Ax = y_\delta.$$

Meanwhile, an alternative method of the L-curve method, which we call it a modified L-curve method, is to find the minimizer of the functional

$$\Psi_\mu = \|Ax(\alpha) - y_\delta\|\|x(\alpha)\|^\mu$$

where $-1/\mu$ is the slope of α^* choesn by a logarithmic L-curve. In this paper we propose a model function approach in the modified L-curve method for the choice of a regularization parameter. The idea is to replace the residual norm and the regularized solution norm with an approximated model function. With such an approach, the computational cost of minimum procedure can be dramatically saved. We present numerical tests to support the reliability of the approach. Finally, the model function approach in modified L-curve method is applied to pool boiling data to reconstruct unknown heat fluxes at the boiling surface.

1. Introduction

In modern numerical analysis on various physical effects, the approximation and solution methods are sophisticated and dependent on some parameters that need to be finely tuned. The Tikhonov regularization, as one of the most widely-spread methods, has been well invested as a parameter-dependent method. In a simplified form, we start the discussion on a numerical solution of discrete ill-posed problems

$$Ax = y \tag{1.1}$$

with a noisy right-hand side y_δ satisfying $\|y_\delta - y\| \le \delta$. The Tikhonov regularization is to find the (global) minimizer of the functional

$$\min_{x\in X} \|Ax - y_\delta\|^2 + \alpha\|x\|^2. \tag{1.2}$$

The performance of the Tikhonov regularization is essentially dependent on the regularization parameter α. If the error bound δ is known, there exist some classic δ-dependent methods in determining the parameter, i.e., the discrepancy principle [3], the balancing principle [11]. In real applications, the accurate error bound δ is usually a priori unknown due to technical reasons. The error-free choice rules are,

2000 *Mathematics Subject Classification.* 65J20, 65M30.

Key words and phrases. Ill-posed problems, l-curve, model function.

in these cases, more promising to be implemented. An important representative of this class of methods is the L-curve method [6, 9]. It is well-accepted as a reliable heuristic method for choosing the regularization parameter. The idea of the L-curve method is based on an inspection of the residual norms of the computed approximations with the norms of the approximations themselves. This is done by plotting $\|x_\alpha^\delta\|$ versus $\|Ax_\alpha^\delta - y^\delta\|$ in a log-log scale for a large range of α values. The overall shape of the graph often looks like the letter "L". The choice of a regularization parameter is focused on the corner, where the vertical line turns to be a horizontal one. Though there is only little theoretical justification of the L-curve method, a lot of publications show that this method still works well from different aspects.

An earlier work in [13] shows that if the curvature of the L-curve method is maximized at $\alpha = \alpha^*$, and if the tangent value of the L-curve method at $\left(\log \|Ax_{\alpha^*}^\delta - y_\delta\|^2, \log \|x_{\alpha^*}^\delta\|^2\right)$ has a slope $-1/\mu$, then a corresponding functional

$$\Psi_\mu(\alpha) = \|Ax_\alpha^\delta - y_\delta\|^2 \|x_\alpha^\delta\|^{2\mu}, \qquad \mu > 0 \tag{1.3}$$

is minimized at the same point $\alpha = \alpha^*$. But no explicit method in computing the local minimum is introduced afterward. Recently, the functional (1.3) has been investigated in [1] where a fixed-point algorithm that determines a point near the L-corner of the maximum curvature has been suggested.

In this paper, we present an efficient model function approach in the modified L-curve method for the choice of regularization parameters. Similar to [1], this approach only needs the computation of the residual and regularized solution norms. With this knowledge, we construct the model function which iteratively approximates the real residual term and the regularized solution term. A corresponding modeled functional will be introduced to replace the original functional in (1.3). Under the framework of the model function approach, the minimization process (1.3) turns to (iteratively) solve a simple quadratic equation. We thus present an algorithm describing the iterative process. We clarify the connection between the modified L-curve method and the model function approach in modified L-curve method with some theoretical analysis.

The paper is organized as follows. In Section 2 we present the basic algorithm as the fast minimum searching substitute. A theoretical analysis on the algorithm will be discussed in Section 3. In Section 4, we will revisit the model function approach in the modified L-curve method and present a linearized form and a safeguard step from the basic algorithm. Numerical tests on large-scale ill-posed problems are shown in Section 5 to show the efficiency of the proposed method. Section 6 will be introduced as a real application of our approach in the pool boiling system on identifying the unknown heat flux. A final Section 7 concluding the context closes the paper.

2. **Basic algorithm**

In this section, we recall the idea of model function in [10, 14].

The standard Tikhonov regularization is to find a global minimizer of the functional

$$\min_{x\in X} J_\alpha(x) := \|Ax - y_\delta\|^2 + \alpha\|x\|^2 \tag{2.1}$$

where $\alpha > 0$ plays the role as the regularization parameter. For a fixed α, (2.1) is equivalent to the following variational form

$$\langle Ax, Ag\rangle + \alpha\langle x, g\rangle = \langle y_\delta, Ag\rangle, \qquad \forall g \in X.$$

By taking $g = x$, the minimal cost functional in (2.1) is alternatively defined as

$$J(\alpha) := J_\alpha(x) = \|Ax - y_\delta\|^2 + \alpha\|x\|^2 = \|y_\delta\|^2 - \|Ax\|^2 - \alpha\|x\|^2. \tag{2.2}$$

The following lemma from [10] will be a starting point in the current context.

Lemma 2.1. [10] *Define the regularized solution $x := x(\alpha)$ here as a function depending on α, the first derivative of $J(\alpha)$ with respect to α is then given by*

$$J'(\alpha) = \|x(\alpha)\|^2. \tag{2.3}$$

We make a fundamental assumption in the model function approach as in [10, 14]. By assuming locally $\|Ax\|^2 \approx T\|x\|^2$ in (2.2), we actually arrive at

$$J(\alpha) + \alpha J'(\alpha) + TJ'(\alpha) \approx \|y^\delta\|. \tag{2.4}$$

Since $J(\alpha)$ is a function of α which is problem dependent and not known a priori, we use a simple function to approximate the properties of $J(\alpha)$. The basic idea is to define a specified function, called a model function, $m(\alpha)$ as a substitute of $J(\alpha)$. Then, by putting $m(\alpha)$ in (2.4), we get

$$m(\alpha) + (\alpha + T)m'(\alpha) \approx \|y_\delta\|^2,$$

which is actually an ODE equation for the parameter α. As in [14], a reasonable choice of the model function satisfying the specific ODE equation is

$$m(\alpha) := \|y_\delta\|^2 + \frac{C}{\alpha + T}. \tag{2.5}$$

C, T are constants to be determined in the iteration. $m(\alpha)$ here performs as a local approximation to $J(\alpha)$. A detailed discussion of the properties of the model function for the discrepancy principle can be found in [10, 14].

As a natural result of Lemma 2.1, the first derivative of the model function $m(\alpha)$ can be used to approximate the first derivative of $J(\alpha)$, i.e.,

$$m'(\alpha) = -\frac{C}{(\alpha + T)^2} \approx J'(\alpha) = \|x(\alpha)\|^2.$$

The approximated residual norm $\|Ax(\alpha) - y_\delta\|^2$ will also be presented by the model function $m(\alpha)$ as

$$m(\alpha) - \alpha m'(\alpha) \approx \|Ax(\alpha) - y_\delta\|^2.$$

In the modified L-curve method, the original functional Ψ_μ is defined as

$$\Psi_\mu(\alpha) = \|Ax(\alpha) - y_\delta\|^2\|x(\alpha)\|^{2\mu}. \tag{2.6}$$

By introducing a model function $m(\alpha)$, Ψ_μ can be (locally) estimated by an approximated substitute $\Psi_{C,T,\mu}$ as

$$\begin{aligned}\Psi_\mu(\alpha) \approx \Psi_{C,T,\mu}(\alpha) &= (m(\alpha) - \alpha m'(\alpha))(m'(\alpha))^\mu \\ &= \left(\|y_\delta\|^2 + \frac{C}{\alpha+T} + \frac{\alpha C}{(\alpha+T)^2}\right)\left(\frac{-C}{(\alpha+T)^2}\right)^\mu. \quad (2.7)\end{aligned}$$

The original problem to find the local minimizer of $\Psi_\mu(\alpha)$ reduces to (iteratively) find the minimizer of $\Psi_{C,T,\mu}(\alpha)$. The only problem is the computation of constants C, T. In fact, as in [14], the constants can be easily calculated within the knowledge of residual norm and regularized solution norm, i.e.,

$$\begin{cases} m(\alpha_k) = \|y^\delta\|^2 + \frac{C_k}{\alpha_k+T_k} = J(\alpha_k) = \|Ax(\alpha_k) - y_\delta\|^2 + \alpha\|x(\alpha_k)\|^2; \\ m'(\alpha_k) = -\frac{C_k}{(\alpha_k+T_k)^2} = J'(\alpha_k) = \|x(\alpha_k)\|^2; \end{cases} \quad (2.8)$$

or more precisely,

$$C_k = -\frac{(\|Ax(\alpha_k)\|^2 + \alpha_k\|x(\alpha_k)\|^2)^2}{\|x(\alpha_k)\|^2}, \qquad T_k = \frac{\|Ax(\alpha_k)\|^2}{\|x(\alpha_k)\|^2}. \quad (2.9)$$

We get, hence, the basic algorithm on the model function approach in the modified L-curve method as follows.

Algorithm 1 (Basic Algorithm) Model function approach in modified L-curve

Input: $\epsilon > 0$, y_δ, A, $\mu > 0$.

1: Choose initial guess $\alpha_1 > \alpha_*$.
2: **Do**
3: Solve $(A^TA + \alpha_k I)x = A^T y_\delta$.
4: Update C_k and T_k from (2.8) or (2.9), construct the corresponding model function

$$m_k(\alpha) = \|y_\delta\|^2 + \frac{C_k}{\alpha + T_k}.$$

5: Insert $m_k(\alpha)$ into (2.7), update α_{k+1} as the minimizer of $\Psi_{C_k,T_k,\mu}(\alpha)$, set $k := k + 1$.
6: **While** $\left|\frac{\alpha_{k+1}-\alpha_k}{\alpha_k}\right| \le \epsilon$.
7: Return x, α_k as the stopping rule fulfilled regularized solution x_S and α_S.

The updating of α_{k+1} in the Algorithm 1 is rather easy. As we can see, in each iteration, α_{k+1} satisfies

$$\Psi'_{C_k,T_k,\mu}(\alpha_k) = 0,$$

which is equivalent to finding the solution α_{k+1} to

$$2\mu\|y_\delta\|^2(T_k+\alpha)^2 + (2C_k + 4\mu C_k)(T_k+\alpha) - (2+2\mu)C_kT_k = 0. \quad (2.10)$$

The quadratic equation (2.10) has, in principle, two solutions. From numerical experience, the smaller one is the next iteration α_{k+1}. In Section 4, we introduce a linearized form to avoid the quadratic computation of (2.10).

Figure 1 illustrates the performance of Algorithm 1 with the test problem *shaw*(100) from [8]. Dashed line is the exact value of Ψ_μ (2.6) with $\mu = 1$.

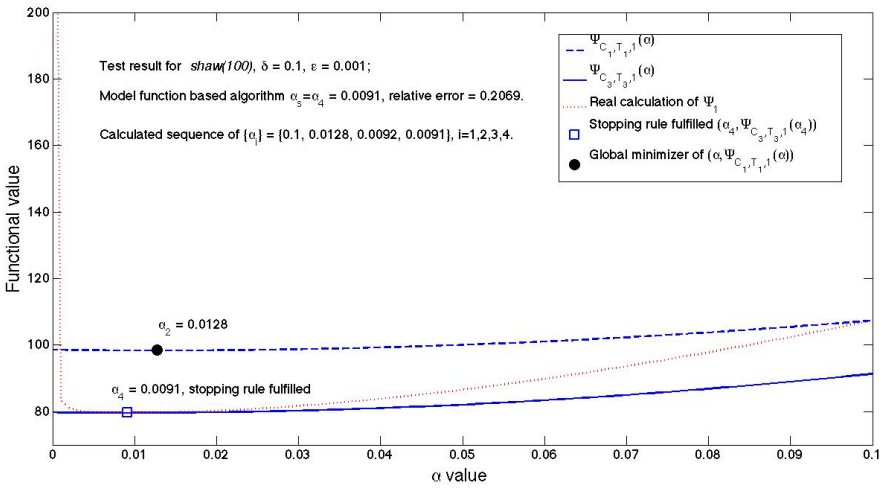

FIGURE 1. Procedure of fast minimization algorithm with $\delta = 0.1$, $\alpha_1 = 0.1$ and $\epsilon = 0.001$. Dashed line is the exact calculation of Ψ_1 with 100 equal-distance discrete points in $[10^{-5}, 10^{-1}]$. Grey dotted line is the $\Psi_{C,T,1}(\alpha)$ under $\alpha_1 = 0.1$ indicated as $\Psi_{C_1,T_1,1}(\alpha)$. $\bullet$ is the global minimizer of $(\alpha, \Psi_{C_1,T_1,1}(\alpha))$ where $\alpha_2 = 0.0128$. Dark solid line is the $\Psi_{C,T,1}$ under α_3 indicated as $\Psi_{C_3,T_3,1}(\alpha)$. $\square$ is the point $(\alpha_4, \Psi_{C_3,T_3,1}(\alpha_4))$ fulfilling the stopping rule. Thus $\alpha_S = \alpha_4 = 0.0091$.

We plot the corresponding $\Psi_1(\alpha)$ under an equal-distance discrete set $\{\alpha_k\}_{k=1}^{100} \in [10^{-5}, 10^{-1}]$. The dashed line $\Psi_1(\alpha)$ represents a benchmark for the computation of Algorithm 1. Algorithm 1 starts with initial guess $\alpha_1 = 0.1$. After generating $\Psi_{C,T,\mu}$ based on α_1, $\mu = 1$ (dotted line in Figure 1), we immediately arrive at $\alpha_2 = 0.0128$ as the minimizer of $\Psi_{C_1,T_1,1}(\alpha)$. Then next iteration will start from α_2. The algorithm will stop immediately after 3 iteration as in this example with $\epsilon = 0.001$; $\alpha_4 = 0.0091$, minimizer of $\Psi_{C_3,T_3,1}(\alpha)$ (solid line in Figure 1), will be chosen as it fulfills the stopping criteria. From the illustrated figure, α_4 is very close to the local minimizer of original $\Psi_1(\alpha)$. Numerically, the sequence $\{\alpha_k\}_{k=1}^{100}$ yields a minimum value of $\Psi_1(\alpha)$ when $\alpha = 0.009$ in this particular example. At the same time, L-curve suggests a similar regularization parameter as $\alpha = 0.0072$. The relative error for Algorithm 1 is 0.2069, whereas, the L-curve obtains a relative error of 0.2142.

3. **Model function approach in the modified L-curve method**

In this section, we analyze the model function approach in the modified L-curve method using the singular value decomposition.

First, we give a brief introduction of the preliminary results and notations. Let $A \in C^{m,n}$ be a matrix of rank r, then there exists a singular value decomposition

of A such that

$$A = U\Sigma V^*, \quad \Sigma = \begin{pmatrix} \Sigma_r & 0 \\ 0 & 0 \end{pmatrix},$$

where unitary matrices $U \in C^{m,m}$, $V \in C^{n,n}$ and $\Sigma \in R^{m,n}$, $\Sigma_r = \mathrm{diag}(\sigma_1, \ldots, \sigma_r)$ with $\sigma_1 \geq \sigma_2 \geq \cdots \geq \sigma_r > 0$. The $\{\sigma_i\}$ are singular values of A; the i-th column vectors u_i, v_i of U and V, respectively, are the left and right singular vectors corresponding to σ_i.

Then, the right-hand side y_δ can be represented as

$$y_\delta = \sum_{i=1}^{m} y_i u_i, \quad \text{where } y_i = \langle u_i, y_\delta \rangle, \quad i = 1, \ldots, m$$

and

$$x(\alpha) = \sum_{i=1}^{r} \frac{\sigma_i y_i}{\sigma_i^2 + \alpha} v_i. \tag{3.1}$$

Correspondingly, we have

$$Ax(\alpha) = \sum_{i=1}^{r} \frac{\sigma_i^2 y_i}{\sigma_2 + \alpha} u_i; \tag{3.2}$$

and

$$Ax(\alpha) - y_\delta = -\left(\sum_{i=1}^{r} \frac{\alpha y_i}{\sigma_i^2 + \alpha} u_i + y_\perp \right), \qquad y_\perp = \sum_{i=r+1}^{m} y_i u_i. \tag{3.3}$$

To analyze the model function approach in the modified L-curve method, we define

$$\rho(\alpha) := \|Ax(\alpha) - y_\delta\|^2 \quad \text{and} \quad \eta(\alpha) := \|x(\alpha)\|^2 \tag{3.4}$$

and

$$\rho_M(\alpha) := m(\alpha) - \alpha m'(\alpha) \quad \text{and} \quad \eta_M(\alpha) := m'(\alpha). \tag{3.5}$$

In this context, we approximate $\rho(\alpha) \approx \rho_M(\alpha)$ and $\eta(\alpha) \approx \eta_M(\alpha)$ respectively.

We recall the technical lemma from [10].

Lemma 3.1. [10] *The function $x(\alpha)$ is infinitely differentiable at every α and its derivative $x^{(n)}(\alpha) \in X$, for each $n \geq 1$, is the unique solution w to the following equation*

$$\langle Aw, Ag \rangle + \alpha \langle w, g \rangle = -n \langle x^{(n-1)}(\alpha), g \rangle \qquad \textit{for all } g \in X. \tag{3.6}$$

By analyzing the properties of ρ, ρ_M, η, η_M, we arrive at the following lemma.

Lemma 3.2. *If $\rho(\alpha)$, $\eta(\alpha)$ are defined by (3.4), then*

$$\frac{d\eta}{d\rho} = -\frac{1}{\alpha}.$$

Meanwhile, the model function based $\rho_M(\alpha)$ and $\eta_M(\alpha)$ in (3.5) obtains the same properties where

$$\frac{d\eta_M}{d\rho_M} = -\frac{1}{\alpha}.$$

Proof. The first assertion is shown in some references, i.e., [1], [9], [13] using the singular value decomposition.

We give here an alternative proof with a direct variation form. From the definition of ρ, η and Lemma 3.1, we have

$$\frac{d\rho}{d\alpha} = 2\langle Ax - y_\delta, Ax'\rangle \quad \text{and } \frac{d\eta}{d\alpha} = 2\langle x, x'\rangle.$$

The Tikhonov regularization is equivalent to the following form

$$\langle Ax, Ag\rangle + \alpha\langle x, g\rangle = \langle y_\delta, Ag\rangle, \quad \forall g \in X.$$

Taking $g = x'$, we get

$$\langle Ax - y_\delta, Ax'\rangle = -\alpha\langle x, x'\rangle.$$

The first assertion is proven.

The same properties of ρ_M and η_M is easy to derive since

$$\rho_M(\alpha) = \|y_\delta\|^2 + \frac{C}{\alpha + T} + \frac{\alpha C}{(\alpha + T)^2} \quad \text{and} \quad \eta_M(\alpha) = -\frac{C}{(\alpha + T)^2}.$$

Respectively, we have

$$\frac{d\rho_M}{d\alpha} = -2\frac{\alpha C}{(\alpha + T)^3} \quad \text{and} \quad \frac{d\eta}{d\alpha} = \frac{2C}{(\alpha + T)^3}.$$

□

Remark 3.3. Lemma 3.2 shows that $\rho_M(\alpha)$ and $\eta_M(\alpha)$ model the relation between original residual term $\rho(\alpha)$ and solution norm $\eta(\alpha)$ exactly. Moreover, η_M as a function of ρ_M is decreasing and strictly convex.

Recall the definition of $\Psi_\mu(\alpha)$ and $\Psi'_\mu(\alpha)$

$$\begin{aligned}
\Psi_\mu(\alpha) &= \|Ax(\alpha) - y_\delta\|^2 \|x(\alpha)\|^{2\mu} = \rho(\alpha)\eta^\mu(\alpha); \\
\Psi'_\mu(\alpha) &= \eta^\mu(\alpha)\eta'(\alpha)\left[\mu\frac{\rho(\alpha)}{\eta(\alpha)} + \frac{\rho'(\alpha)}{\eta'(\alpha)}\right].
\end{aligned}$$

Without loss of generality, from Lemma 3.1, we assume for $\alpha > 0$

$$\begin{aligned}
\eta(\alpha) &= \|x(\alpha)\|^2 > 0; \\
\eta'(\alpha) &= 2\langle x(\alpha), x'(\alpha)\rangle = -2\|Ax'(\alpha)\|^2 - 2\alpha\|x'(\alpha)\|^2 < 0.
\end{aligned}$$

Thus the solutions of $\Psi'_\mu(\alpha) = 0$ also satisfy

$$\mu\frac{\rho(\alpha)}{\eta(\alpha)} + \frac{\rho'(\alpha)}{\eta'(\alpha)} = 0.$$

By Lemma 3.2, we can conclude that

Theorem 3.4. *The modified L-curve method is equivalent to the stationary equation*

$$\mu\|Ax(\alpha^*) - y_\delta\|^2 = \alpha^*\|x(\alpha^*)\|^2.$$

The minimization of Ψ_μ is thus equivalent to finding the α^* such that the stationary equation is satisfied.

Similar observation can also be found in [1]. From Theorem 3.4, we can introduce an important safeguard rule for the model function approach in the modified L-curve method.

Lemma 3.5. *Assume following inequality*

$$\mu\|Ax(\alpha_k) - y_\delta\| < \alpha_k\|x(\alpha_k)\|^2 \tag{3.7}$$

holds, in each step in Algorithm 1 the functional $\Psi_{C_k,T_k,\mu}(\alpha)$ is locally strict increasing at point α_k.

Proof. We start with

$$\Psi_{C_k,T_k,\mu}(\alpha) = \left(\|y_\delta\|^2 + \frac{C_k}{T_k+\alpha} + \frac{\alpha C_k}{(T_k+\alpha)^2}\right)\left(\frac{-C_k}{(T_k+\alpha)^2}\right)^\mu.$$

The derivative of $\Psi_{C_k,T_k,\mu}(\alpha)$ can be derived as

$$\begin{aligned}(\Psi_{C_k,T_k,\mu}(\alpha))' &= \left(\frac{-2\alpha C_k}{(T_k+\alpha)^3}\right)\left(\frac{-C_k}{(T_k+\alpha)^2}\right)^\mu \\ &\quad -2\mu\left(\|y_\delta\|^2 + \frac{C_k}{(T_k+\alpha)} + \frac{\alpha C_k}{(T_k+\alpha)^2}\right)\frac{(-C_k)^\mu}{(T_k+\alpha)^{2\mu+1}}. \end{aligned}\tag{3.8}$$

Take $\alpha = \alpha_k$ and insert the definition of C_k, T_k, we have

$$(\Psi_{C_k,T_k,\mu}(\alpha_k))' = \frac{2\|x(\alpha_k)\|^{2+2\mu}}{\|Ax(\alpha_k)\|^2 + \alpha_k\|x(\alpha_k)\|^2}\left(\alpha_k\|x(\alpha_k)\|^2 - \mu\|Ax(\alpha_k) - y_\delta\|^2\right).$$

From the assumption, we conclude that

$$(\Psi_{C_k,T_k,\mu}(\alpha_k))' > 0.$$

□

Corollary 3.6. *Lemma 3.7 shows that, in each iteration of Algorithm 1, starting from an initial guess α_1 satisfying the safeguard rule (3.9), we can always generate a monotonic successive sequence $\{\alpha_i\}$ such that $\alpha_{k+1} < \alpha_k$ and each α_i in the sequence satisfies the safeguard rule.*

Lemma 3.7. *Assume following inequality*

$$\mu\|Ax(\alpha_k) - y_\delta\| < \alpha_k\|x(\alpha_k)\|^2 \tag{3.9}$$

holds, in each step in Algorithm 1 the strict monotonicity of the sequence $\{\alpha_k\}$ *is valid, i.e.* $\alpha_{k+1} < \alpha_k$*, if there exists an* $\alpha_{k+1} > 0$ *s.t.* $\Psi_{C_k,T_k,\mu}(\alpha_{k+1}) = 0$.

Proof. We start with

$$\Psi_{C_k,T_k,\mu}(\alpha) = \left(\|y_\delta\|^2 + \frac{C_k}{T_k+\alpha} + \frac{\alpha C_k}{(T_k+\alpha)^2}\right)\left(\frac{-C_k}{(T_k+\alpha)^2}\right)^\mu.$$

The derivative of $\Psi_{C_k,T_k,\mu}(\alpha)$ can be derived as

$$\begin{aligned}(\Psi_{C_k,T_k,\mu}(\alpha))' &= \left(\frac{-2\alpha C_k}{(T_k+\alpha)^3}\right)\left(\frac{-C_k}{(T_k+\alpha)^2}\right)^\mu \\ &\quad -2\mu\left(\|y_\delta\|^2 + \frac{C_k}{(T_k+\alpha)} + \frac{\alpha C_k}{(T_k+\alpha)^2}\right)\frac{(-C_k)^\mu}{(T_k+\alpha)^{2\mu+1}} \\ &= 2\frac{(-C_k)^\mu}{(T_k+\alpha)^{2\mu+3}}[-\mu\|y_\delta\|^2(T_k+\alpha)^2 \\ &\quad -(2\mu C_k + C_k)(T_k+\alpha) + C_kT_k(\mu+1)]. \end{aligned} \tag{3.10}$$

Algorithm 1 yields an updated α_{k+1} satisfying $(\Psi_{C_k,T_k,\mu}(\alpha_{k+1}))' = 0$.

Since $\alpha > 0$, $C_k < 0$ and $T_k > 0$, we obtain $\frac{(-C_k)^\mu}{(T_k+\alpha)^{2\mu+3}} > 0$.

Thus, we define an auxilinary function as follows

$$\Lambda(\alpha) = -\mu\|y_\delta\|^2(T_k+\alpha)^2 - (2\mu C_k + C_k)(T_k+\alpha) + C_kT_k(\mu+1).$$

It is clear that α_{k+1} also satisfies $\Lambda(\alpha_{k+1}) = 0$.

Take $\alpha = \alpha_k$ and insert the definition of C_k, T_k, we have

$$\Lambda(\alpha_k) = \frac{\left(\|Ax(\alpha_k)\|^2 + \alpha_k\|x(\alpha_k)\|^2\right)^2}{\|x(\alpha_k)\|^4}\left(\alpha_k\|x(\alpha_k)\|^2 - \mu\|Ax(\alpha_k) - y_\delta\|^2\right).$$

From the assumption, we conclude that

$$\Lambda(\alpha_k) > 0.$$

Since $\Lambda(\alpha_{k+1}) = 0$ and $-\mu\|y_\delta\|^2 < 0$, the property of the quadratic form $\Lambda(\alpha)$ suggests the monotonicity of $\alpha_{k+1} < \alpha_k$ (if $\alpha_{k+1} > 0$ exists) since we always take the smaller updated α_{k+1} in the numerical implementation. □

The reason we call $\{\alpha_i\}$ a successive sequence is that the quadratic updating form (2.10) may not have solutions for a particular μ. We formulate the result as following lemma.

Lemma 3.8. *There exists a $\mu > 0$ such that step 5 in Algorithm 1 exists a minimizer to $\Psi_{C_k,T_k,\mu}(\alpha)$. But not for all μ there always exists a minimizer.*

Proof. As can be seen in the previous section, the step 5 in Algorithm 1 or (2.10), there exists a minimizer if and only if

$$(1+2\mu)^2 C_k^2 + 2\mu\|y_\delta\|^2(2+2\mu)C_k T_k \geq 0.$$

Recall the definition of C_k and T_k in (2.9), the existence of the minimizer is equivalent to

$$\begin{aligned} -\frac{(\|Ax(\alpha_k)\|^2+\alpha_k\|x(\alpha_k)\|^2)^2}{\|x(\alpha_k)\|^2}+ & \\ (4\mu+4\mu^2)\frac{\|Ax(\alpha_k)\|^2\|Ax(\alpha_k)-y_\delta\|^2-\alpha_k^2\|x(\alpha_k)\|^4}{\|x(\alpha_k)\|^2} & \leq 0. \end{aligned}$$

Define an auxiliary function as follows

$$\begin{aligned} \Theta(\mu) &= -\frac{(\|Ax(\alpha_k)\|^2+\alpha_k\|x(\alpha_k)\|^2)^2}{\|x(\alpha_k)\|^2} \\ &\quad +(4\mu+4\mu^2)\frac{\|Ax(\alpha_k)\|^2\|Ax(\alpha_k)-y_\delta\|^2-\alpha_k^2\|x(\alpha_k)\|^4}{\|x(\alpha_k)\|^2}. \end{aligned}$$

It is obvious that $\Theta(0) < 0$ and $\Theta(\mu)$ is continuous over μ. Moreover, as we can see

$$\begin{aligned} \Theta'(\mu) &= (4+8\mu)\frac{\|Ax(\alpha_k)\|^2\|Ax(\alpha_k)-y_\delta\|^2-\alpha_k^2\|x(\alpha_k)\|^4}{\|x(\alpha_k)\|^2}; \\ \Theta''(\mu) &= 8\frac{\|Ax(\alpha_k)\|^2\|Ax(\alpha_k)-y_\delta\|^2-\alpha_k^2\|x(\alpha_k)\|^4}{\|x(\alpha_k)\|^2}. \end{aligned}$$

From the preliminary information, we have

$$\begin{aligned} \|Ax(\alpha_k)-y_\delta\|^2 &= \alpha_k^2\sum_{i=1}^r\frac{\|y_i\|^2}{(\sigma_i^2+\alpha_k)^2}+\|y_\perp\|^2; \\ \|Ax(\alpha_k)\|^2 &= \sum_{i=1}^r\frac{\sigma_i^4\|y_i\|^2}{(\sigma_i^2+\alpha_k)^2}; \\ \alpha_k^2\|x(\alpha_k)\|^4 &= \alpha_k^2\left(\sum_{i=1}^r\frac{\sigma_i^2\|y_i\|^2}{(\sigma_i^2+\alpha_k)^2}\right)^2. \end{aligned}$$

Then

$$\begin{aligned}\|Ax(\alpha_k)\|^2\|Ax(\alpha_k)-y_\delta\|^2 &= \left(\alpha_k^2\sum_{i=1}^{r}\frac{\|y_i\|^2}{(\sigma_i^2+\alpha_k)^2}+\|y_\perp\|^2\right)\sum_{i=1}^{r}\frac{\sigma_i^4\|y_i\|^2}{(\sigma_i^2+\alpha_k)^2}\\ &\geq \alpha_k^2\sum_{i=1}^{r}\frac{\|y_i\|^2}{(\sigma_i^2+\alpha_k)^2}\sum_{i=1}^{r}\frac{\sigma_i^4\|y_i\|^2}{(\sigma_i^2+\alpha_k)^2}\\ &\geq \alpha_k^2\left(\sum_{i=1}^{r}\frac{\sigma_i^2\|y_i\|^2}{(\sigma_i^2+\alpha_k)^2}\right)^2=\alpha_k^2\|x(\alpha_k)\|^4.\end{aligned}$$

Thus, both $\Theta'(\mu)$ and $\Theta''(\mu)$ are positive over μ for $\mu>0$. $\Theta(\mu)$ is an increasing and convex function with $\Theta(0)<0$. The lemma is thus proven. □

Lemma 3.8 seems to suggest a scheme to choose μ adaptively so that the quadratic updating form always has a solution. But in the modified L-curve method, the $-1/\mu$ should be chosen as the slope of α^* by the logarithmic L-curve, which is a fixed value. In order to avoid the nonexistence situation, we will discuss a refined updating form in the next section.

4. **Model function approach revisited**

In Section 3, we analyze the properties of Algorithm 1. As shown in Lemma 3.8, the quadratic form (2.10) may not provide a solution for a fixed μ. Instead of changing μ, a better way is to replace the corresponding quadratic updating form into a linear one.

As we can see from (2.10), α_{k+1} satisfies

$$2\mu\|y_\delta\|^2(T_k+\alpha_{k+1})^2+(2C_k+4\mu C_k)(T_k+\alpha_{k+1})-(2+2\mu)C_kT_k=0$$

or

$$(2C_k+4\mu C_k)(T_k+\alpha_{k+1})=(2+2\mu)C_kT_k-2\mu\|y_\delta\|^2(T_k+\alpha_{k+1})^2.$$

Moreover, from the monotonicity of $\{\alpha_i\}$ sequence as in Corollary 3.6, we insert $\alpha_{k+1}<\alpha_k$ into the previous equation and obtain

$$(2C_k+4\mu C_k)(T_k+\alpha_{k+1})>(2+2\mu)C_kT_k-2\mu\|y_\delta\|^2(T_k+\alpha_k)^2.$$

Since C_k is always negative, the inequality yields

$$\alpha_{k+1}<-T_k+\frac{(2+2\mu)C_kT_k}{2C_k+4\mu C_k}-\frac{2\mu\|y_\delta\|^2(T_k+\alpha_k)^2}{2C_k+4\mu C_k}.$$

So we just introduce a contraction factor ω_l $(0<\omega_l<1)$ such that

$$\alpha_{k+1}\approx\omega_l\left(-T_k+\frac{(2+2\mu)C_kT_k}{2C_k+4\mu C_k}-\frac{2\mu\|y_\delta\|^2(T_k+\alpha_k)^2}{2C_k+4\mu C_k}\right). \tag{4.1}$$

The linearized form (4.1) will always provide an approximated minimizer compared with the original quadratic updating form (2.10).

We thus obtain a refined algorithm based on the linearized updating form (4.1) and the safeguard rule (3.9).

Algorithm 2 (Modified Algo.) Model function approach in modified L-curve

Input: $\epsilon > 0$, y_δ, A, $\mu > 0$, $0 < \omega < 1$.

1: Choose initial guess $\alpha_1 > \alpha_*$.
2: **Do**
3: Solve $(A^T A + \alpha_k I)x = A^T y_\delta$.
4: Update C_k and T_k from

$$\begin{cases} m_k(\alpha_k) = \|y^\delta\|^2 + \frac{C_k}{\alpha_k + T_k} = J(\alpha_k) \\ m_k'(\alpha_k) = -\frac{C_k}{(\alpha_k + T_k)^2} = J'(\alpha_k) = \|x(\alpha_k)\|^2 \end{cases}$$

5: Update α_{k+1} as the approximated minimizer in (4.1) with a fixed contraction factor ω.
6: if $\mu\|Ax(\alpha_{k+1}) - y_\delta\|^2 > \alpha_{k+1}\|x(\alpha_{k+1})\|^2$ **End While**; or else set $k := k + 1$.
7: **While** $\left|\frac{\alpha_{k+1} - \alpha_k}{\alpha_k}\right| \leq \epsilon$.
8: Return x, α_k as the stopping rule fulfilled regularized solution x_S and α_S.

5. Performance evaluations in simulation

In this section, we compare the model function approach in the modified L-curve method (Algorithm 1 and Algorithm 2) with the original L-curve method. In our experiments, we focus on the numerical cases under the large scale situation in order to access the efficiency of the different methods.

Large scale problems usually appear from science and engineering applications, for example inverse helioseismology, computerized tomography etc. The feature of large scale problems is that the matrix factorization is prohibitive or expensive to implement. Then some classical matrix inverse methods like SVD will not be a good option. Take $A_{m\times n}$ matrix as an example, the regular inverse of SVD takes a basic cost of $O(mn^2)$ steps. Then consider the classical Tikhonov regularization in ill-posed problems with the discrepancy principle, the computational cost will be $O(p(m+n))O(mn^2)$ time with a number p indicating the discrete parameters that must be tried.

The conjugate gradient method is a standard tool for solving large linear systems and linear least squares problems. We consider the conjugate gradient least square (CGLS) method in later computation to solve some linear systems appearing in the Tikhonov regularization. The computational cost for one CGLS step is $O(3n + 2m)$ [2]. Detail discussion on related algorithms can be found in [12]. A survey that covers large scale ill-posed problems can be found in [5]. An application of CGLS to the Tikhonov regularization is investigated in [4].

The estimation quality is measured by the relative error to the original clean data, which is defined by the norm of error over that of the clean data in L_2 norm. The lower the relative error, the better the quality of reconstruction.

The performance of L-curve will be run under the *Regularization toolbox* [7] and its updated large-scale descendant *Moore tools* [8].

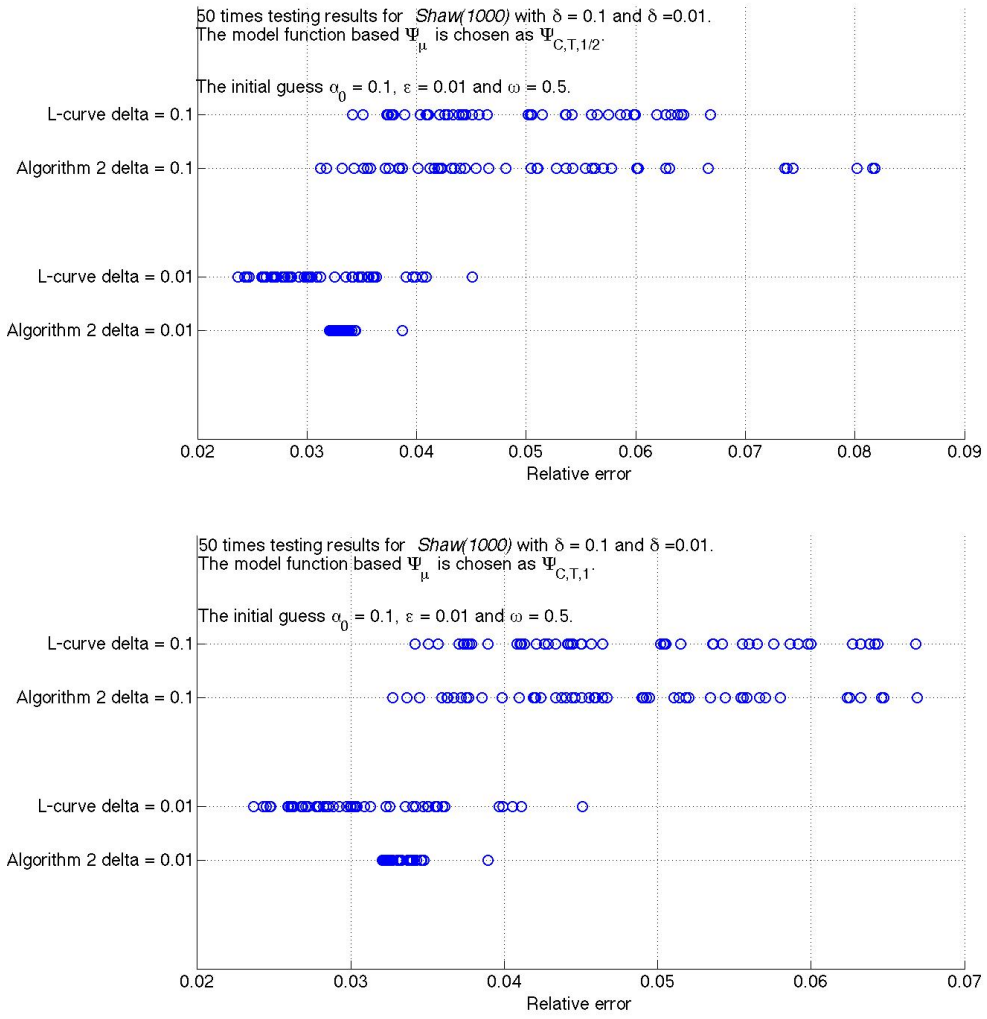

FIGURE 2. Upper: $\mu_1 = 1/2$; lower: $\mu_1 = 1$. $Shaw(1000)$ test with initial guess $\alpha_1 = 0.1$ and $\epsilon = 0.01$. x role is the relative error for each test. In each figure, the upper first two lines are performed under $\delta = 0.1$ and the rest two lines are performed under $\delta = 0.01$. Each circle in the figures indicates the relative error led by one reconstruction obtained via respective methods (L-curve or Algorithm 2); the smaller relative error the better.

The first example is based on the test function $shaw(n)$ [8] with $n = 1000$. It is a discretization of the Fredholm first kind integral equation

$$\int_{-\frac{\pi}{2}}^{\frac{\pi}{2}} k(s,t)f(t)dt = g(s), \quad s \in [-\frac{\pi}{2}, \frac{\pi}{2}],$$

where the kernel and the solution are given by

$$k(s,t) = (\cos(s) + \cos(t))^2 \left(\frac{\sin(u)}{u}\right)^2, \quad u = \pi(\sin(s) + \sin(t)),$$
$$f(t) = a_1 e^{-c_1(t-t_1)^2} + a_2 e^{-c_2(t-t_2)^2},$$
$$a_1 = 2, \quad a_2 = 1, \quad c_1 = 6, \quad c_2 = 2, \quad t_1 = 0.8, \quad t_2 = -0.5.$$

The kernel and the solution are discretized by a simple collocation with n points to produce the operator matrix A and the solution vector $x^\dagger$. Then the discrete right-hand side is computed by $y = Ax^\dagger$.

We now try to solve

$$Ax = y$$

where the right-hand side is known as y_δ with $\|y_\delta - y\| \leq \delta$. As usual, the perturbed right-hand side is generated as

$$y_\delta = Ax^\dagger + \sigma \|e\|_2^{-1} e,$$

where e is a normal distribution with zero mean and unit standard deviation.

The CGLS process used here contains 20 iterations with 10^{-52} as the termination tolerance on the residual. Comparison between the model function approach in the modified L-curve method (Algorithm 2) and the L-curve method is run under the same conditions. The corresponding results are shown in Figure 2 (upper) for $\mu_1 = 1/2$ and Figure 2 (lower) for $\mu_1 = 1$.

As we can see from the figures, for a larger $\mu = 1$, the numerical results are more stable and better than the result by $\mu = 1/2$. Both μ present good results compared with the L-curve method.

The second test is based on the function $baart(n)$ [8] with $n = 1000$. It is a discretization of the Fredholm equations

$$\int_0^\pi e^{s\cos t} f(t) dt = 2\frac{\sin s}{s}, \qquad s \in [0, \frac{\pi}{2}].$$

The test solution is $f(t) = \sin(t)$. The corresponding results are shown in Figure 3 (upper) for $\mu = 1/2$ and Figure 3 (lower) for $\mu = 1$. Similar to the previous example, the numerical result for $\mu = 1$ is more stable, but a smaller $\mu = 1/2$ produces better quality in comparison with the L-curve method. It seems that sometimes a smaller μ produces better resolutions.

The comparison of computational time between the model function approach in the modified L-curve method (Algorithm 1, Algorithm 2) and the L-curve method can be seen in Table 1 and 3. An information on the average iteration is also delivered there. For different noise level, the model function approach in the modified L-curve method (Algorithm 1) usually takes less than 5 iteration, which means we only need to solve less than 5 time of the large scale linear systems. The linearized algorithm (Algorithm 2) takes more iteration steps, which is a reasonable compromise against the original quadratic form. In real application, the reader can use either methods to balance the efficiency or the accuracy. Of course, a smaller μ or a combined quadratic-linearized algorithm is also preferred

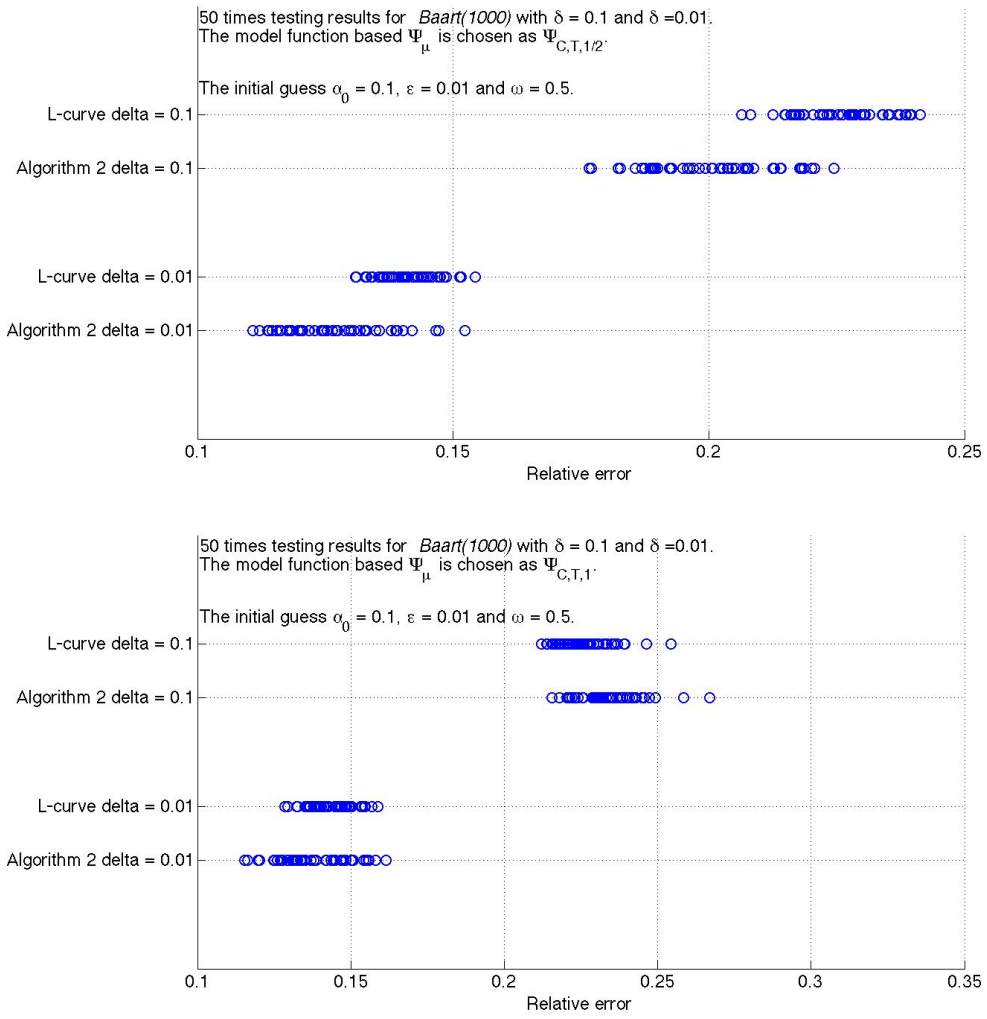

FIGURE 3. Upper: $\mu = 1/2$; lower: $\mu = 1$. $Baart(1000)$ test with initial guess $\alpha_1 = 0.1$ and $\epsilon = 0.01$. x role is the relative error for each test. The upper first two lines are performed under $\delta = 0.1$ and the two lines are performed under $\delta = 0.01$. Each circle in the figures indicates the relative error led by one reconstruction obtained via respective methods (L-curve or Algorithm 2); the smaller relative error the better.

but will not be taken into account in current context. Both tables show the efficiency of the proposed method.

TABLE 1. Computation information for Algorithm 1 (A1) and L-curve (Average data over 50 times tests; Comp Time means the computational time, units in second)

	Noise Level	A1 Iteration	A1 Comp Time	L-curve Comp Time
$Shaw(1000)$				
$\mu = 1$	$\delta = 0.1$	3	2.1656	27.2446
	$\delta = 0.01$	4	2.6524	26.6567
$\mu = 1/2$	$\delta = 0.1$	3	2.2133	27.9781
	$\delta = 0.01$	4	2.6663	26.9823
$Baart(1000)$				
$\mu = 1$	$\delta = 0.1$	3	1.9712	29.3494
	$\delta = 0.01$	4	2.3736	28.0244
$\mu = 1/2$	$\delta = 0.1$	3	1.9368	28.5860
	$\delta = 0.01$	3.16	1.9980	28.3343

TABLE 2. Computation information for Algorithm 2 (A2) and L-curve (Average data over 50 times tests; Comp Time means the computational time, units in second)

	Noise Level	A2 Iteration	A1 Comp Time	L-curve Comp Time
$Shaw(1000)$				
$\mu = 1$	$\delta = 0.1$	9	5.5119	27.8922
	$\delta = 0.01$	13	7.6556	27.8343
$\mu = 1/2$	$\delta = 0.1$	8	4.8413	27.2615
	$\delta = 0.01$	11	6.4592	27.2238
$Baart(1000)$				
$\mu = 1$	$\delta = 0.1$	3	1.9233	28.3110
	$\delta = 0.01$	8	4.2840	28.0008
$\mu = 1/2$	$\delta = 0.1$	3	1.9188	28.2624
	$\delta = 0.01$	7	3.7922	27.9048

6. **Application to the heat flux reconstruction problem in pool boiling**

In this section, we discuss an interesting problem arising from pool boiling, which is a very important process in engineering. Applications are the production of process steam in vapor generators, the distillation of fluids in rectification columns, or the rapid cooling of steel in metallurgical quenching processes. Its importance has provided the incentive for theoretical and experimental investigations on the the macro, the meso and micro as well as the molecular scale over the past decades. Among all studies to boiling processes, the reconstruction of the unmeasurable local boiling heat fluxes is fundamental but crucial. For this purpose, high resolution measurement techniques and corresponding data processing methods are necessary.

In recent years, boiling experiments at a single artificial nucleation site have been conducted at TU Darmstadt [15]. The experiments were carried out on

TABLE 3. Computation comparison for Algorithm 1 (A1) and Algorithm 2 (A2) (Average data over 50 times tests, noise level $\delta = 0.1$), $e(\alpha) = \alpha\|x(\alpha)\|^2 - \mu\|Ax(\alpha) - y_\delta\|^2$.

	A1 iteration	Value of $e(\alpha)$ with $\alpha = \alpha_S$
$\mu = 1/2$	4	$e(\alpha_S) = 7.23 \times 10^{-6}$
$\mu = 1$	4	$e(\alpha_S) = 4.60 \times 10^{-5}$
$\mu = 3$	5	$e(\alpha_S) = 2.58 \times 10^{-5}$
$\mu = 5$	6	$e(\alpha_S) = 7.36 \times 10^{-6}$

	A2 iteration	Value of $e(\alpha)$ with $\alpha = \alpha_S$
$\mu = 1/2$	8	$e(\alpha_S) = 0.0031$
$\mu = 1$	9	$e(\alpha_S) = 0.0085$
$\mu = 3$	10	$e(\alpha_S) = 0.0253$
$\mu = 5$	10	$e(\alpha_S) = 0.0413$

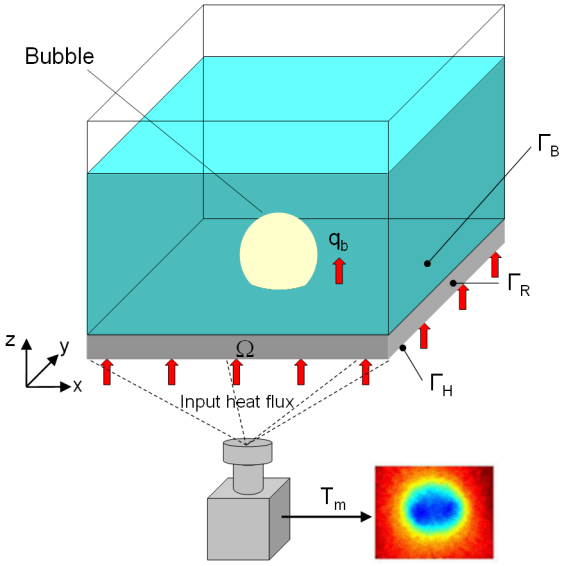

FIGURE 4. Schematic representation of a single-bubble nucleate boiling experiment.

a 50 μm thick stainless steel thin heater and the temperature field at the back side of the heater was observed with a high-speed infrared camera (cf. Figure 4). In the related work [16], an iterative regularization strategy, obtained by applying the conjugate gradient for optimization and the L-curve method for regularization, was proposed for the estimation of the local boiling heat flux from measured temperature field. This solution approach has also been successfully applied to another pool boiling problem, where an irregular computational domain was considered [17].

6.1. **Problem formulation.** We consider the inverse heat conduction problem (IHCP) defined in a 3D domain Ω with boundary $\partial\Omega = \Gamma_H \cup \Gamma_B \cup \Gamma_R$ (cf. Figure

4) [16]. Γ_H, Γ_B and Γ_R denote the heated, the boiling and the adiabatic boundary of Ω, respectively.

The temperature $T(\mathbf{x}, t)$ inside Ω satisfies the linear heat conduction equations,

$$\mathbb{S} = \begin{cases} \frac{\partial T(\mathbf{x},t)}{\partial t} &= a\Delta T(\mathbf{x},t), \quad (\mathbf{x},t) \in \Omega \times [0,t_f], \\ T(\mathbf{x},0) &= T_0(\mathbf{x}), \qquad \mathbf{x} \in \Omega, \\ -\lambda\frac{\partial T(\mathbf{x},t)}{\partial n} &= q_h(\mathbf{x},t), \quad (\mathbf{x},t) \in \Gamma_H \times [0,t_f], \\ -\lambda\frac{\partial T(\mathbf{x},t)}{\partial n} &= q_b(\mathbf{x},t), \quad (\mathbf{x},t) \in \Gamma_B \times [0,t_f], \\ -\lambda\frac{\partial T(\mathbf{x},t)}{\partial n} &= 0, \qquad (\mathbf{x},t) \in \Gamma_R \times [0,t_f], \end{cases}$$

where λ and a are the known constant thermal conductivity and diffusivity coefficients. T_0, q_h and q_b are the initial and boundary conditions. The final time is denoted by t_f and $\frac{\partial T(\mathbf{x},t)}{\partial n}$ denotes the Neumann condition along the specified boundaries.

The inverse problem corresponds to the estimation of the unknown heat flux q_b at the boiling surface Γ_B from the measured transient temperature field T_m on the back of the thin heater Γ_H governed by the system $\mathbb{S}$. The system $\mathbb{S}$ maps $(T_0, q_h, q_b) \to T_m$, where T_m is the final observation temperature.

The original system $\mathbb{S}$ can be decomposed into two systems

$$\mathbb{S}1 = \begin{cases} \frac{\partial T1(\mathbf{x},t)}{\partial t} &= a\Delta T1(\mathbf{x},t), \quad (\mathbf{x},t) \in \Omega \times [0,t_f], \\ T1(\mathbf{x},0) &= T_0(\mathbf{x}), \qquad \mathbf{x} \in \Omega, \\ -\lambda\frac{\partial T1(\mathbf{x},t)}{\partial n} &= q_h(\mathbf{x},t), \quad (\mathbf{x},t) \in \Gamma_H \times [0,t_f], \\ -\lambda\frac{\partial T1(\mathbf{x},t)}{\partial n} &= 0, \qquad (\mathbf{x},t) \in \Gamma_B \times [0,t_f], \\ -\lambda\frac{\partial T1(\mathbf{x},t)}{\partial n} &= 0, \qquad (\mathbf{x},t) \in \Gamma_R \times [0,t_f], \end{cases}$$

and

$$\mathbb{S}2 = \begin{cases} \frac{\partial T2(\mathbf{x},t)}{\partial t} &= a\Delta T2(\mathbf{x},t), \quad (\mathbf{x},t) \in \Omega \times [0,t_f], \\ T2(\mathbf{x},0) &= 0, \qquad \mathbf{x} \in \Omega, \\ -\lambda\frac{\partial T2(\mathbf{x},t)}{\partial n} &= 0, \qquad (\mathbf{x},t) \in \Gamma_H \times [0,t_f], \\ -\lambda\frac{\partial T2(\mathbf{x},t)}{\partial n} &= q_b(\mathbf{x},t), \quad (\mathbf{x},t) \in \Gamma_B \times [0,t_f], \\ -\lambda\frac{\partial T2(\mathbf{x},t)}{\partial n} &= 0, \qquad (\mathbf{x},t) \in \Gamma_R \times [0,t_f]. \end{cases}$$

System $\mathbb{S}1$ maps the known data set $(T_0, q_h) \to T1_m$; system $\mathbb{S}2$, on the other hand, maps the unknown heat flux $q_b \to T2_m$. The relation between different temperatures is $T_m = T1_m + T2_m$. As we can see, $T1_m(\mathbf{x}, t)$ is the result from system $\mathbb{S}1$, it can be precomputed even without knowledge of $T_m(\mathbf{x}, t)$.

Thus, in the corresponding inverse problem, the main work will focus on the system $\mathbb{S}2$. We define here the corresponding linear operator as A and rewrite system $\mathbb{S}2$ as

$$Aq_b(\mathbf{x},t) = T2_m(\mathbf{x},t) = T_m(\mathbf{x},t) - T1_m(\mathbf{x},t).$$

In reality, $T_m(\mathbf{x}, t)$ often contains some observation error. So the ill-posed problem that we need to handle is

$$Aq_b(\mathbf{x},t) = T2_m^\delta(\mathbf{x},t) = T_m^\delta(\mathbf{x},t) - T1_m(\mathbf{x},t). \tag{6.1}$$

The Tikhonov functional for (6.1) can be written as follows

$$J(\alpha) := \int_0^{t_f} \int_{\Gamma_H} |Aq_b(\mathbf{x},t) - T2_m^\delta|^2 d\mathbf{x}dt + \alpha \int_0^{t_f} \int_{\Gamma_B} |q_b(\mathbf{x},t)| d\mathbf{x}dt. \tag{6.2}$$

In Section 6.2, we consider the solution of the IHCP defined on a crosscut of the 3D domain Ω (cf. Section 6.1) and use the notations in (6.1) and (6.2). The discretization of the original system (6.1) is presented by the standard B-spline systems of time and space separately, i.e.,

$$q_b(\mathbf{x},t) = \sum_{i=1}^{N_s} \sum_{j=1}^{N_t} q_{i,j} \psi_i(\mathbf{x}) \phi_j(t), \tag{6.3}$$

where N_s and N_t are the discretization level for space and time. The reconstructed solution in Tikhonov regularization (6.2) can thus be obtained by a Galerkin method.

In Section 6.3, we apply the proposed solution approach validated in Section 6.2 to the heat flux reconstruction with real measurement data in pool boiling. The unknown boiling heat flux at surface Γ_B is reconstructed by solving a series of 2D IHCPs defined on crosscuts of the 3D domain Ω.

6.2. **A 2D simulation study.** In order to reconstruct the unknown heat flux $q_b(\mathbf{x},t)$, we use the Tikhonov regularization. The regularization parameter α is chosen by the model function approach in the modified L-curve method.

In this case study, the domain is chosen as $\Omega = 1 \times 0.05$ mm^2, the density $\rho = 7900$ kg/m^3, specific heat $c = 520$ J/kgK and thermal conductivity $\lambda = 14.5$ W/mK result in a thermal diffusivity of $a = 3.53 \times 10^{-6}$ m^2/s. The initial and known lower boundary heat flux are $T_0 = 55\ ^\circ C$ and $q_h = 5000$ W/m^2, respectively. The simulation time interval is $t \in [0, 0.05$ s$]$. The observation time step is $\tau = 0.001$ s, i.e., 50 discretized observation time steps in $[0, 0.05$ s$]$.

The exact heat flux (in W/mm^2) is defined as $q_b(\mathbf{x},t) = \alpha(t) \cdot \beta(\mathbf{x})$, $(\mathbf{x},t) \in \Gamma_B \times [0,t_f] = [0,1] \times [0,0.05]$, where $\alpha(t) = 0.1 \sin(100\pi(t-0.02)) + 0.1$ for $t \in [0.015, 0.035]$, zero elsewhere; and $\beta(\mathbf{x}) = \beta(x) = 0.5 \sin(5\pi(0.3 - |x-0.5|)) + 0.5$ for $|x-0.5| \leq 0.4$, zero elsewhere.

The exact temperature T_m is computed from the solution of the direct problem with known q_b on Γ_B using Matlab PDE toolbox [18]. The perturbed data is simulated by adding measurement error to T_m, i.e., $T_m^\delta = T_m + \delta\epsilon$ where δ is 10% noisy level of exact data and ϵ is a uniform distributed random vector with zero mean and variance one.

The discretization level chosen for q_b is $N_s = 25$ and $N_t = 10$. The advantage of the Galerkin method is that some matrices in the discretized Tikhonov regularization can be precomputed. The use of the model function approach in the modified L-curve method will also decrease the computational time significantly.

In this case study, we start the model function approach in the modified L-curve method (Algorithm 2) with similar algorithm parameters as in Section 5, i.e., $\mu = 1$, an initial $\alpha_1 = 10^{-3}$, $\epsilon = 0.01$ and a contraction factor $\omega = 0.5$. The Algorithm 2 will search for the fulfilled α_S at around 2.2×10^{-5} within 5 iterations.

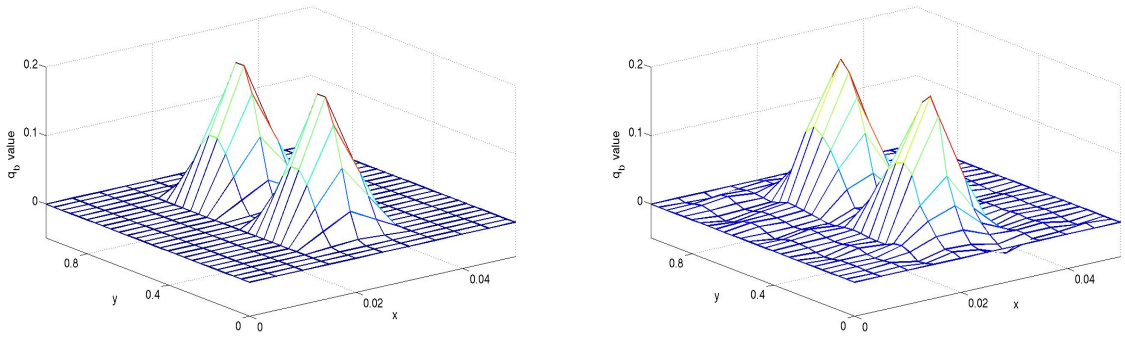

FIGURE 5. The exact q_b for the academic example (left) and the reconstructed q_b by the model function approach in the modified L-curve method (Algorithm 2 with 5 iterations) (right).

The exact data and reconstructed q_b can be found in Figure 5. The result shows the reliability of our proposed algorithm.

6.3. **Pool boiling reconstruction.** We investigate in this section the real problem arising from the pool boiling system, where the thin heater has a thickness of 50μm and the measurement section has a spatial resolution of 152×144 pixel with a pixel size of 16×16 μm. We consider the IHCP solution in the 3D domain $\Omega := 2.416 \times 2.288 \times 0.05$ mm^3. Six unknowns are used for the space discretization in z-direction. 50 time frames of temperature measurements are taken with a sampling frequency of 987 Hz. This translates to a time step size of $\tau \approx 1.013$ ms for the time discretization. As we mentioned in previous section, the reconstruction will consider 152 crosscuts along the x-coordinate and each crosscut corresponds to a 2D IHCP with 144×50 observation data. The reconstructed heat flux will stay with the discretization level of $N_s = 25$ and $N_t = 10$. The initial temperature distribution T_0 is assumed to be non-constant across the foil thickness as the first observation temperature. A known input heat flux $q_h = 5356$ W/m^2 is applied. The material properties have already been given in previous section.

The measured temperature distribution (in K) on the x–y-plane at time frames 24-27 is depicted in Figure 6 which correspond to an emerging single bubble cycle, as confirmed by simultaneous imaging with a high speed camera. The noise of the scanner is 0.13 K (95% of the values are in this range). The signal has an amplitude of about 1.5 K. Thus, the signal to noise ratio is around 11.5. A cold region in the temperature distribution at frame 24 is the result of the activity of an earlier bubble.

The reconstructed surface boiling heat fluxes (in W/mm^2) are shown in Figure 7. They are consistent with those in [16]. It is apparent that the boiling heat flux undergoes a significant change during the emerging bubble cycle and a ring-shaped region of the local heat flux is observed. The peak value of the estimated heat fluxes is nearly 30 times larger than their average value. This moves a step towards the confirmation of the microlayer proposed by Stephan and Hammer [19]. In their theory they predicted that most of the heat during boiling is transferred in

the micro-region of the three-phase contact line by evaporation. The computation was conducted using MacBook Pro Core Duo 2 GHz and the total time added up to ca. 20 minutes. The Tikhonov regularization under the computational framework established here for the 3D IHCP within the pool boiling system will be investigated in a forthcoming paper. The shown results only confirm the reliability of the proposed approach.

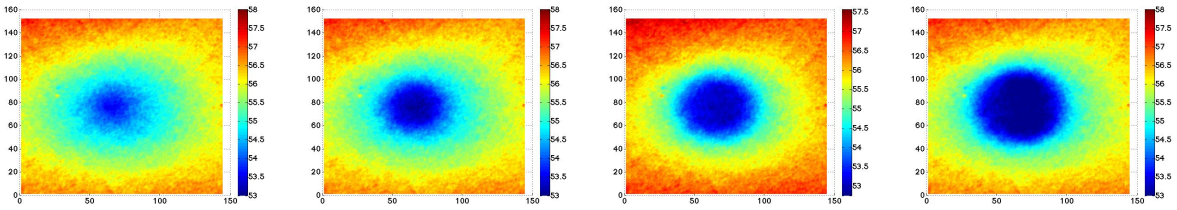

FIGURE 6. The measured temperature field on the back side of the heater; from left to right: Frame 24 - Frame 27.

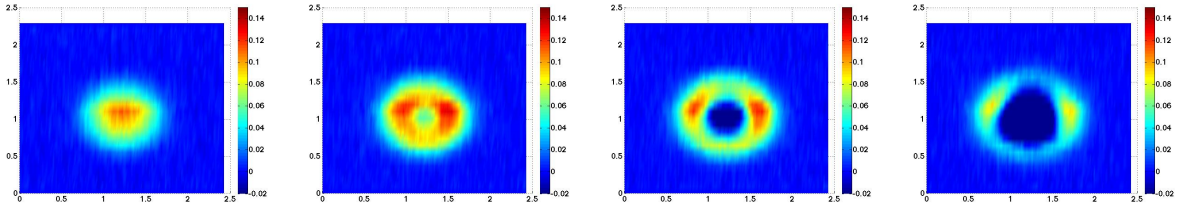

FIGURE 7. The reconstructed surface boiling heat flux; from left to right: Frame 24 - Frame 27.

7. Conclusion

We have demonstrated that the model function approach in the modified L-curve method is a simple yet computationally efficient algorithm for solving ill-posed problems. The procedure is based on the the modified L-curve method by the modeled terms on the residual norm and the solution norm. The resulting functional $\Psi_{C,T,\mu}$ can be easily minimized with respect to a specific μ in a quadratic or a linearized form. To the best of our knowledge, it is also the first time that the model function approach is implemented into a heuristic method.

In our tests, the model function approach in the modified L-curve method produces reconstructed solution with similarly stable and accurate quality with comparison to the L-curve method. The proposed algorithm only takes few computational steps with a fixed initial guess and a specified stopping rule in different numerical examples.

Acknowledgments

The first and third authors are supported by German Science Foundation (DFG) through the research training group GRK 775 and a joint research project on

fundamentals of boiling heat transfer. The second and forth authors are supported by the Austrian Fonds Zur Förderung der Wissenschaftlichen Forschung (FWF), Grant P20235-N18. We also acknowledge to Prof. Stephan and co-workers for giving us access to experimental data [15].

References

[1] Bazán, F. S. V. (2008): *Fixed-point iterations in determining the Tikhonov regularization parameter*, Inverse Problems, **24**, 035001 (15pp).
[2] Björck, A. (1996): *Numerical method for least squares problems*
[3] Engl, H. W., Hanke, M. and Neubauer, A (1996): *Regularization of Inverse Problems*, Dordrecht: Kluwer.
[4] Frommer, A. and Maass, P. (1996) *Fast CG-based methods for Tikhonov-Phillips Regularization*, SIAM J. Sci. Comput., **20**, 1831–1850.
[5] Hanke, M. and Hansen, P. C. (1993): *Regularization methods for large-scale problems*, Surv. Math. Ind., **3**, 253–315.
[6] Hansen, P. C. (1992):*Analysis of discrete ill-posed problems by means of the L-curve*, SIAM Review, **34**, 561–580.
[7] Hansen, P. C. (1994):*Regularization tools: a Matlab package for analysis and solution of discrete ill-posed problems*, Numerical Algorithms, **6**, 1 – 35.
[8] Hansen, P. C.: *Moore tools*, http://www2.imm.dtu.dk/∼pch/.
[9] Hansen, P. C. and O'Leary, D. P. (1993): *The use of the L-curve in the regularization of discrete ill-posed problems*, SIAM J. Sci. Comput., **14**, 1487 – 1503.
[10] Kunisch, K. and Zou, J. (1998): *Iterative choices of regularization parameters in linear inverse problems*, Inverse Problems, **14**, 1247–1264.
[11] Mathé, P. and Pereverzev S.V. (2003): *Geometry of linear ill-posed problems in variable Hilbert scales*, Inverse Problems, **19**, 789–803.
[12] Quarteroni A., Sacco R. and Saleri F. (2000): *Numerical mathematics*, Springer.
[13] Regińska, T. (1996): *A regularization parameter in discrete ill-posed problems*, SIAM J. Sci. Comput., **17**, 740 – 749.
[14] Xie J. and Zou J. (2002): *An improved model function method for choosing regularization parameters in linear inverse problems*, Inverse Problems, **18**, 631–643.
[15] Wagner, E. et al., *Nucleate boiling at single artificial cavities: Bubble dynamics and local temperature measurements*, 6^{th} *International Conference on Multiphase Flow*, Leipzig, Germany, 9–13 July 2007.
[16] Heng, Y., Mhamdi, A., et al., *Identification of boiling heat fluxes in a single-bubble nucleate boiling experiment using a three-dimensional transient heat conduction model*, J. Phys.: Conf. Ser., **135**, 012051.
[17] Heng, Y., Mhamdi, A., P. et al. (2008) *Reconstruction of local heat fluxes in pool boiling experiments along the entire boiling curve from high resolution transient temperature measurements*, Int. J. Heat and Mass Transfer, **51**, 5072–5087.
[18] Cook, Robert D., Malkus, David S., and Plesha, Michael E. (1989), *Concepts and Applications of Finite Element Analysis*, 3rd edition, John Wiley & Sons, New York.
[19] Stephan, P. and Hammer J. (1994), *A new model for nucleate boiling heat transfer*, Wärme- und Stoffübertragung, **30**, 119–125.

[1] AVT-Process Systems Engineering, RWTH Aachen University, Turmstr. 46, D-52064 Aachen, Germany

E-mail address: yi.heng@avt.rwth-aachen.de, adel.mhamdi@avt.rwth-aachen.de.

[2], Johann Radon Institute for Computational and Applied Mathematics, Austrian Academy of Sciences, Altenbergstrasse 69, 4040 Linz, Austria
E-mail address: shuai.lu@oeaw.ac.at, sergei.pereverzyev@oeaw.ac.at.

Correspond to Shuai Lu